Towards More Sustainable Building Based on modified Portland Cements Through Partial Substitution by Engineered Feldspars

E. Enríquez*+[1,2], M. Torres-Carrasco+[2,3], M.J. Cabrera[1], D. Muñoz[1], J. F. Fernández[2]

+These authors contributed equally to this work

[1]Centro tecnológico Vidres, S.L., Ctra. Onda, Km 3.4, 12540 Villareal, Castellón, Spain

[2] Electroceramics Department, Instituto de Cerámica y Vidrio, CSIC, Kelsen 5, 28049, Madrid, Spain.

[3] Materials Science and Engineering Department-IAAB, University Carlos III of Madrid, Avda. Universidad 30, 28911 Leganés, Madrid, Spain

Abstract

Global warming is one of the main problems that facing modern civilization. As buildings consume 40% of total energy, the heating in the cities is a primary concern. Therefore, it seeks to improve sustainable construction materials with better thermal and reflective properties, reducing consumption and heat islands. In this work, mineral and engineered feldspars have been used as partial substitution of white cement, that is widely used in the cladding of façades mainly due to its high whiteness, to improve composites' reflectance and reducing their thermal conductivity. Both feldspars show pozzolanic effect and new composites have superior whiteness and reflectance (>12 %). Moreover, the engineered feldspar avoids the alkali-silica reaction (ASR) effect in spite of its alkaline content. A reduction of heat of > 2 ºC after 6 hours of solar irradiance is demonstrated for engineered feldspar composite resulting in a good alternative for their implementation as exterior insulation and finish systems.

Keywords: cement; feldspar; thermal conductivity; pozzolanity.

1. Introduction

Currently, the impact of the global warming over the planet is an important problem that should be solved immediately. For this purpose, research actions are being carried out in order to control and reduce heat island effects in the cities [1,2]. Particularly, new procedures and materials for facings are used to produce sustainable buildings which allows reducing the energy consumption for acclimatization [2–5]. Cement is one of the main construction materials and often it serves as

*Corresponding author. Tlf:+34 91 735 58 40; Ext 922076. Fax: +34 91 735 58 43. E-mail address: esther@icv.csic.es (E. Enríquez)

decorative element for façades. Nowadays, it exists a constant need to develop cementitious based materials that contribute respectfully with environment under economics and energetic requirements for the buildings [6,7]. Given this scenario, cement has presented in recent years a remarkable evolution that has banished the concept of multipurpose material and, today, it is possible to speak of specialized cement. One classified variety is the white Portland cement (WPC) that currently is used as avant-garde material able to satisfy the building requirements, presenting high mechanical resistances, in addition to its aesthetic and decorative properties that give it an added value.

In the Portland cement production process, if the final product is to be White Portland cement, materials should have the least possible amount of ferrous and manganese cations. The production process is done at higher temperature than of an ordinary Portland cement (OPC). White cement can be used for the same uses as gray OPC with the exceptions of building that are in contact with sea water, as it erodes easier [8]. As previously mentioned, it is preferred to use white cement when an aesthetic use is pursued, as is the case of buildings where the mortars or concrete are visible [9].

In order to obtain cementitious materials with thermal efficiency to reduce the energy consumption, different types of materials from by-industrial waste or from natural origin are added. The European regulations in force (UNE-EN 197-1:2011) clearly state the allowed cement additions in Europe, such as blast furnace slag [10,11], fly ash [12], silica fume [10,13], limestone [13] and pozzolans [14,15]. The term pozzolanic is generally used to define materials which are cementitious by themselves, having a chemical composition that, at room temperature and combined with lime in the presence of water, forms stable and insoluble compounds which behave as hydraulic conglomerates [17]. The $Ca(OH)_2$ required for the pozzolanic reaction can come directly from the hydrated lime or from the hydration of the Portland cement. The use of pozzolanic materials can be justified from different points of view, as technical, economic or environmental. The environmental policies seek to reduce the accumulation of waste, thus prioritizing the recycling of waste and/or industrial by-products for use in the manufacture of cement. However, the use of traditional pozzolans (fly ash, blast furnace slag) tends to decline in recent years due to the intention of reducing the landscape and environmental impact that this exploitation generates. In addition, new goals are looking for obtaining new functionalities in cements materials which provide them an added value, such as, a good whiteness, high reflectivity and low thermal conductivity. Thus, it is necessary to look for available materials with pozzolanic capacity having good mechanical and durable properties.

In spite of the great availability of feldspars, since it is the most abundant material on earth, their use as cement additives is quite limited due to their large alkaline content. Alkaline contents could favor the alkali-silica reactions (ASR) degrading the cement pieces due to the expansions phenomena. This effect is a very important problem that involves great amount of research works, where the alkalis release in pore solution and the mortars expansion is study by the influence of several parameters, such as humidity, pH, temperature, etc [16,17]. Conversely, feldspars chemical composition includes Ca, Si and Al cations and, therefore, pozzolanic properties could be expected and, in addition, it can provide other functionalities, as whiteness, hardness, etc. Recently, engineered feldspar as new glass-ceramic material based mainly on anorthite feldspar ($CaSi_2Al_2O_8$) was designed [3]. It possesses a unique micro-nanostructure that consisted on anorthite microcrystals surrounded by a nanostructure/glass region. The large amount of grain boundaries enlarged the phonon scattering and, as consequence, improves the thermal, optical and electrical properties of the material. This material, in form of ceramic tiles, provides high solar reflectivity and low thermal diffusivity, allowing an improvement in the energy saving of the buildings, up to 22 %, when it is used in linings both outside and in the inner.

Therefore, the aim of this work is to develop white cements with improved thermal and optical properties to enlarge thermal efficiency in buildings. For this purpose, white cement pastes will be partially substituted by two different kinds of feldspars, a natural feldspar based on albite ($NaAlSi_3O_8$) and a synthetized feldspar (engineered feldspar). The feldspar substitution proportions effect on the pozzolanic activity, alkalis released in pore solution, thermal and optical properties will be studied. Moreover, thermal efficiency of developed cement based materials will be evaluated by using a solar simulator set-up. The obtained results will compare the effect of both feldspars additions (natural and synthetized).

2. Experimental procedure

2.1 Materials and processes

White Portland cement (WPC, 42.5R) was used in this study. The chemical composition of this material is given in Table 1. The particle size distribution was D_{10} =1.31 μm, D_{50} = 11.04 μm and D_{90} = 38.4 μm, and the specific surface area (BET) was 1.65 m^2/g.

The feldspar raw materials were: a) mineral feldspar (hereinafter M) based sodium plagioclase and b) engineered plagioclase feldspar (hereinafter E). The E feldspar was prepared following the standard ceramic processing for the tile industry described in previous works [3], in which powder

94 form is obtained by industrial alumina ball milling for 4 hours. The powder was oven dried thereafter.
95 The mineral feldspar is also milled and dried following the same procedure. The chemical
96 composition of both materials is show in Table 1 and their physical properties are shown in Table
97 2. The particle size distribution of the M and E feldspars are D_{10} = 1.33 µm, D_{50} = 5.86 µm, D_{90} =
98 18.7 µm, and D_{10} = 0.83 µm, D_{50} = 2.43 µm, D_{90} = 6.91 µm, respectively, and the specific surface
99 area (BET) was 2.42 m^2/g and 6.21 m^2/g for M and E feldspars, respectively. Cement pastes with
100 substitution of 15 wt. % and 25 wt. % of white cement were dry mixed in a turbula mixer to obtain
101 a homogenous mix. Pastes were prepared by using distilled water with a L/S = 0.35. In all cases,
102 the L/S ratio was the same to work in the same conditions.

103 **Table 1.** Chemical composition by XRF of used raw materials.

Material	Equivalent oxides (wt. %)											
	CaO	SiO_2	Al_2O_3	MgO	Fe_2O_3	Na_2O	K_2O	TiO_2	P_2O_5	ZrO_2	SO_3	LOI
White Cement	63.0	14.5	3.45	0.58	0.18	0.17	0.27	0.07	0.04	-	2.03	15.7
E feldspar	11.8	47.9	21.4	0.57	0.23	4.58	1.65	0.11	0.004	7.31	-	
M feldspar	0.61	69.0	19.2	0.05	0.04	10.4	0.20	0.03	0.02	-	-	

104

105 **Table 2.** Physical properties of used raw materials.

Material	Thermal conductivity (W/mK)*	Whiteness (*L)	Reflectance (%)
White cement	0.59	87.7	62.8
E feldspar	0.35	98.1	100.0
M feldspar	-	95.7	84.1

106 * Thermal conductivity was measured in a cement paste cured 28 days and in a E feldspar ceramic. M feldspar
107 thermal conductivity was not able to be measured because of their powder nature.
108

109 ### 2.2 Characterization Methods

110 *Pozzolanic activity (Saturated Lime Solution test, SLS):* feldspars pozzolanicity was assessed with
111 an accelerated chemical method not described in the standards, although based on the
112 pozzolanicity test for pozzolanic cements recommended in European legislation [18]. The test
113 involves placing 1 g of sample in 75 mL of a saturated lime solution (SLS) at 40 ˚C for a pre-
114 established test time. After the reaction time lapses, solutions were filtered and 0.02M EDTA-

titrated to determine its CaO concentration. The amount (%) of lime fixed by the mineral or engineered feldspar is then calculated as the difference between the reference concentration (17.68 mmol/L) and the concentration in the last solution.

Fratini test: the pozzolanicity test of Fratini method was found in the European regulations (UNE-EN 196-5) for pozzolanic cements [19,20]. It consisted in the evaluation of the concentration of lime in a solution containing cement with the different percentages of addition of the incorporated residue. In this case, as the main difference with the SLS test, the pozzolanicity test for pozzolanic cements in contact with distilled water was evaluated. The pozzolanic cements will be a consequence of the incorporation of feldspar as partial replacement of cement. The methodology was as follows: 20 grams of the pozzolanic cement was mixed with 100 mL of distilled and decarbonated water. The mixture was stirred vigorously to homogenize as much as possible and kept in an oven at 40ºC. The test ages included in the regulations were 8 and 15 days. After the reaction periods, the filtered solution was evaluated in an analogous way to the method used to determine the pozzolanic activity of the used feldspars.

Structural characterization of the composites and the raw materials was carried out with X ray diffraction (XRD) technique in a diffractometer Bruker D8 Advance with Cu Kα radiation, 40kV and 40mA, during the aging of the samples. The crystalline phases were identified by the comparison with the JCPDS patterns. Fourier Transform Infrared spectroscopy (FTIR) of samples was carried out by FTIR spectrometer Perkin Elmer, Spectrum 100 in transmittance in the range of 400 – 4000 cm^{-1} by attenuated total reflectance (ATR) of the powders.

Alkali release in pore solution: The alkali release can be the responsible of the Alkali-silica Reactions (ASR) in cements, even for low alkaline content. Therefore, the feldspars presence can be a source of alkalis which could favor the ASR. To study this phenomenon, the alkali release in pore solution of cements has been analyzed at 1, 7 and 30 days. With this purpose, cement samples with 0, 15 and 25 wt. % of feldspars substitution in cement pastes have been milled and solved in distilled water at 1g/100ml concentration. The solutions were kept in agitation for the time indicated at room temperature. After the experiment, pH of each solution was measured, and the liquid was separated from the cement powder by centrifugation (20 min at 6000 rpm) in order to analyze the alkali ions released by plasma spectrometry technique (ICP-OES) in a IRIS ADVANTAGE equipment from Termo Jarrel Ash.

Chemical analysis of raw materials was carried out by means plasma spectrometry technique (ICP-OES), using a IRIS ADVANTAGE de Termo Jarrel Ash equipment which has a radio frequency

source of 40, 68 MHz, diffraction network type "Echelle", and solid state detector of load transfer (CID).

Reflectance measurements were carried out by a Perkin Elmer Lambda 950 spectrophotometer with an integration sphere to obtain the total reflectance (diffuse and direct reflectance) in the solar spectrum range (300-2500) nm with a step of 3 nm. Spectralon® Diffuse Reflectance Standards was used as pattern, which is considered as 100% of reflectance in these measurements.

*CIE L*a*b* coordinates*, the most common uniform color space, were measured by a colorimeter Konica Minolta, Spectra Magic NX, with Color Data Software CM-S100w. L* measures from black to white (0-100), a* measures from green to red and b* from blue to yellow. Therefore, the whiteness of samples can be obtained with the combination of the three coordinates.

Thermal conductivity measurements of samples were obtained at room temperature by means of DTC-25 Conductivity meter of TA Instrument using the guarded heat flow method.

Solar simulation experiments: Solar simulation measurements consist in irradiating the surface sample with the simulator lamp with the aim to obtain the thermal behavior of samples in the entire solar spectrum with the corresponding intensity in each wavelength. Samples surfaces were irradiating during 5 min. The achieved temperature on surface was simultaneously measured with a thermal infrared camera and at the same time, temperature transmitted through the sample at the rear part was measured by means a thermocouple placed in the opposite size of the tile and connected to a multimeter. The data obtained by the multimeter and the thermocamera was processed by designed and commercial software, respectively. Therefore, it was possible to obtain heating curves in both sides of the sample with rather high resolution, which gives information about the reflective capacity and the in situ heat transfer through the sample, related with the thermal diffusivity. The experimental setup was previously reported [3]. The solar simulation experiments were performed by a LCS-100 solar simulator (Lasing S.A.) with a Xenon lamp of 100W. The simulator possesses an AM1.5G filter (applied to the Standard G-173-03 with 1.5 air mass) that reproduces the solar spectrum with one sun equivalent power which allows measuring the reflective effect of the solar radiation on the samples. The solar filter is 81011-LCS with 2” square AM0 filter mounted in frame. In addition, the solar simulation includes an AM1,5G spectral correction filter which shapes the light output to closely match the total (direct and diffuse) solar spectrum on the Earth’s surface, at a zenith angle of 48.23 (ASTM 892). This provides a Class A irradiance spectrum suitable for photovoltaic testing. The thermal properties were measured by means of a thermal infrared camera FLIR E30 with an image resolution of 160x120 pixels and a temperature range of

-20 to 350 ºC with 0.1 ºC of thermal resolution; and with a PT100 thermocouple connected to a multimeter Keithley 2410-1100V, in voltage and current ranges of 0–100 V and 0–21 mA, respectively. The thermocouple system was calibrated using the cold focus method.

Cement application for facade coating: With the aim of checking the efficiency of the cement composites, a cement application was carried out by coating a building brick with the different composites simulating a coating for façades. The coatings were made with pure cement, 25 wt. %. of mineral feldspar and 25 wt. % of engineered ceramic feldspar. The thickness of the composites coatings was 0.40 ± 0.05 cm. Then, the same thermal characterization carried out for pastes was also realized for these application samples (thermal conductivity and sun simulator experiments). The optical characterization was not carried out due to its effect is the same when the paste is deposited over the brick.

3. Results and discussion

3.1 Pozzolanic properties of the used feldspars

In Figure 1 the pozzolanic capacity of the raw feldspars is represented. The pozzolanic capacity is determined as the fixation of lime by the use of an accelerated chemical method [21–24]. It is observed that both feldspars particles possess pozzolanic activity when reacting with a saturated solution of calcium hydroxide, where the worst values exceeded 20 % of fixed calcium hydroxide. As a comparison, fly ash used as an addition to cement has a pozzolanic capacity below 5 % at first ages and around 40 % at 28 days [19]. Thus, feldspars pozzolanic activity is ≥ 50 % at ages of 7 days. Moreover, engineered feldspar is superior in pozzolanic activity than mineral one. It is important to highlight the differences in the pozzolanic capacity of each used material, where it is necessary to take into account several factors, such as the nature and proportion of the active phases, the reactive SiO_2 content and the particle size. The greater pozzolanic activity of feldspars is relates to its content in the acid oxides (SiO_2 + Al_2O_3). However, in spite of the lower content of these acid oxides in E feldspar in comparison with M feldspar, the pozzolanic activity is greater. This difference is related to the higher Ca^{2+} content and the lower particle size of E feldspar against M feldspar since, when the particle size is very small, it favors the pozzolanic activity of the material because of its direct relation with the specific surface area that, as seen before, is larger for E feldspar and, therefore, with the accessible contact surface for the reaction with $Ca(OH)_2$.

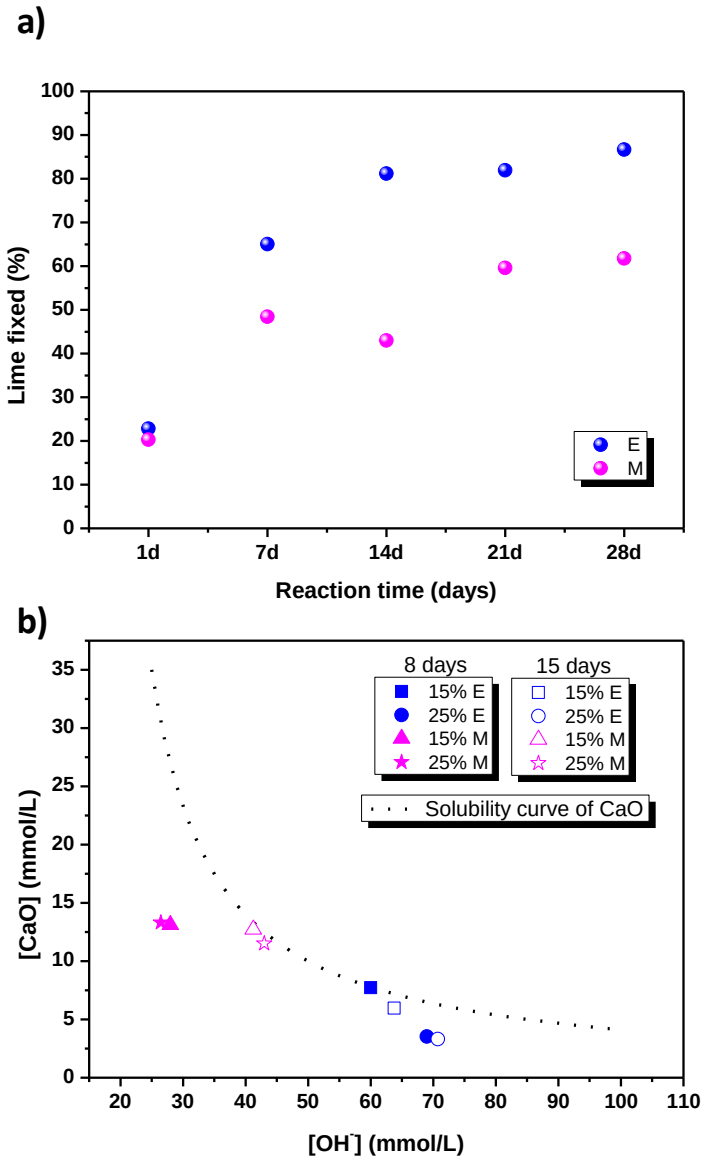

Figure 1. a) Lime fixed by mineral feldspar (pink color) and engineered feldspar (blue color) over time (1, 7, 14, 21 and 28 days); **b)** pozzolanicity test for cements compositions with 15 and 25 wt. % cement substitution by feldspars at 8 days (filled symbols) and 15 days (hollow symbols). In all cases, the cements compositions were below the solubility curve of CaO that indicates their pozzolanic behavior.

According to the results obtained from the pozzolanic activity of each used materials, mixtures were prepared at 15 and 25 wt. % of feldspar substitution for white cement and their pozzolanic behavior was evaluated by the use of Fratini test (UNE-EN 196-5). In Figure 1b it is observed that all these compositions present a pozzolanic behavior. According to European Standard 197-1, for a cement to be considered pozzolanic, it must comply with the pozzolanicity test, i.e. the point obtained after the valorization of calcium and hydroxide ions is below the curve of saturation concentration of the

calcium oxide for a reaction time of 8 days and otherwise, at the age of 15 days. In all the evaluated systems are observed that the addition of 15 and 25 wt. % of these feldspars originates a cementitious material with pozzolanic activity, although it exists differences between the pozzolanicity of the cements relate to the feldspar nature.

The solid reaction products obtained after the reaction between the saturated solution of lime and the natural and engineered feldspars, for the different ages of the test, were dried in an over at 60˚C for 24 hours for further characterization by FTIR and XRD in order to evaluate the hydrated phases formed and, from here, the kinetics of the pozzolanic reaction. Figure 2 shows the FTIR spectra of the raw M and E feldspars and their respective pozzolanic reaction products (SLS tests) at the ages of 1, 7, 14, 21 and 28 days. In the FTIR spectra corresponding to the M feldspar (see Figure 2a), a very intense IR absorption band located around 993 cm^{-1} is observed, mainly associated with Si-O stretching vibrations of the SiO_4 groups. As the pozzolanic reaction assay evolves over time, the M feldspar interacts with the saturated calcium solution and the IR absorption bands corresponding to the departure feldspar start to show slight differences, for instance in the IR band shift. The main IR band, located at 993 cm^{-1}, undergoes a shift towards lower wavenumbers. This is indicative of the formation of a silicon-rich gel, similar to C-S-H gel in Portland cement pastes, mainly because M feldspar has a composition rich in SiO_2 which produces larger depolymerization [25–27]. At the age of 28 days, the IR band is around 979 cm^{-1}, which reveals the existence of a pozzolanic activity of Mineral feldspar. In other words, the reactive silica present in its composition would be available to react with the portlandite when it will be mixed with cement, forming the C-S-H gel.

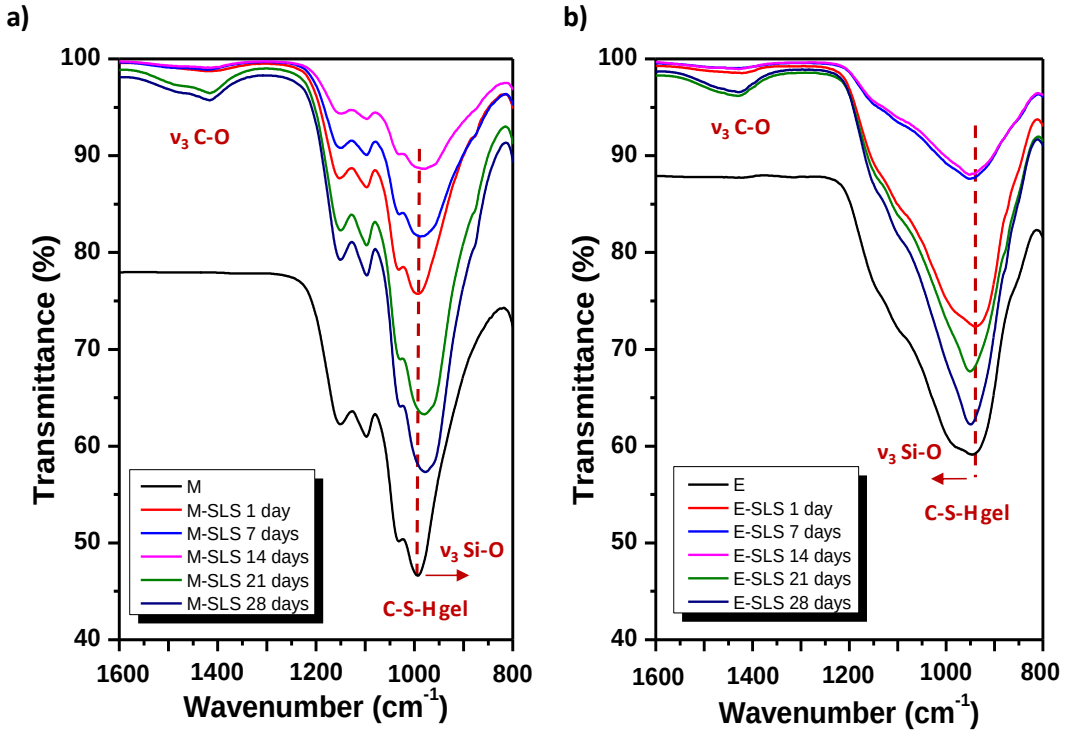

Figure 2. a) Spectra FTIR region between 1600-800 cm^{-1} of Mineral feldspar before and after the reaction with the saturated solution of lime at different ages (1, 7, 14, 21 and 28 days); **b)** FTIR spectra of engineered material before (black line) and after the reaction with the saturated solution of lime at different ages (1, 7, 14, 21 and 28 days).

The same effect is observed in the pozzolanic reaction for the engineered feldspar (see Figure 2b). However, in this case, the main IR absorption band is located around 946 cm^{-1} (lower wavenumbers than in the mineral feldspar) and IR band shifts toward larger wavenumbers, because its chemical composition is different as regards the SiO_2 and CaO content (lower content than M feldspar, see Table 1). Nevertheless, the net IR band shift indicates the gel formation. Thus, it is demonstrated that both feldspars are able to generate gel. In addition, as the pozzolanic reactions evolve over time, it is observed how, regardless of the type of studied feldspar, a new IR absorption band appears at advanced ages of reaction, especially at 21 and 28 days, located around 1430 cm^{-1}, which corresponds to the presence of carbonates of calcite type (C-O asymmetric stretching vibrations) that has been generated over time [28].

By XRD it is possible to observe, in Figure 3, the different phases present after the test of the saturated lime solution (SLS) at the different ages of the study, comparing it with the starting material in both feldspars. Mineral feldspar (see Figure 3a) presents diffraction peaks

corresponding to quartz (JCDPS 87-2096) and albite (JCDPS 9-0466). As the reaction time with the saturated solution of lime evolves (7, 14, 21 and 28 days), new crystalline phase appears at low diffraction angles in addition of the crystalline phases of the M feldspar. The diffraction peak located around 11.1 ˚2θ, corresponds to the presence of a hydrated aluminosilicate of sodium (A), potassium and calcium (JCDPS 47-1870) and the second one, located at 2-theta values ≈ 11.7 ˚2θ, corresponds to the presence of a hydrated carboaluminate (C) (JCDPS 41-0219) (see Figure 3b). Both crystalline phases appear due to the reaction produced between the calcium of the saturated solution of lime with the mineral feldspar. In addition, a slight carbonation of the material appears induced by the action of CO_2 in the medium.

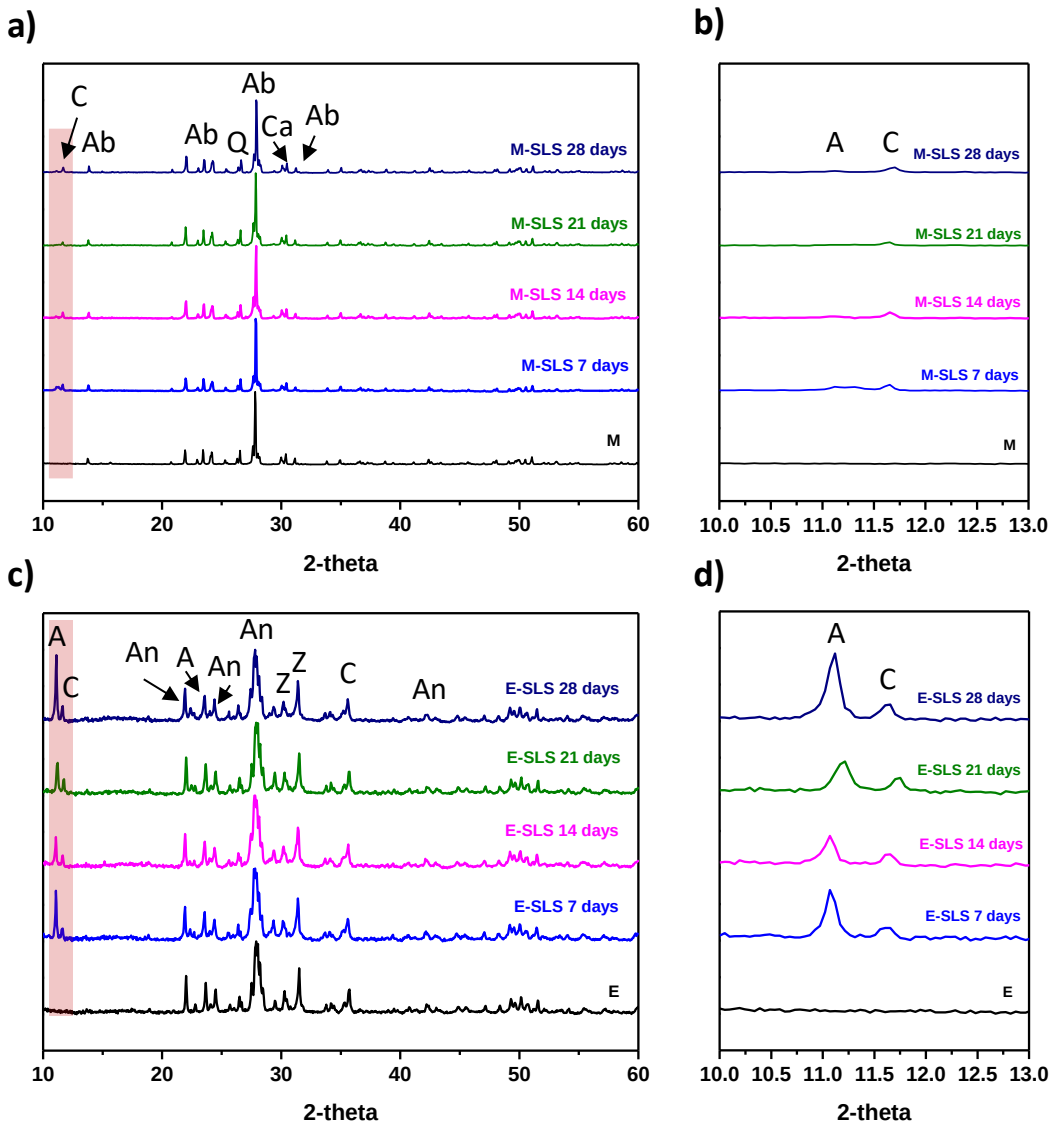

Figure 3. a) XRD diffractogram of M feldspar before (black line) and after the reaction with the saturated solution of lime at different ages (7, 14, 21 and 28 days). The main phases present of the natural feldspar are quartz (Q) and albite (Ab); **b)** diffractogram region between 10-13º 2θ where the presence of aluminosilicate (A) and carboaluminates (C) is shown; **c)** XRD pattern of E feldspar

before (black line) and after the reaction with the saturated solution of lime at different ages (7, 14, 21 and 28 days). In this case, the main phases present are anorthite (An) and zircona (Z); **d)** diffractogram region between 10-13˚ 2θ where the appearance of the new phases of aluminosilicate (A) and carboaluminates (C) are present after the reaction with the saturated solution of lime.

In Figure 3c, the diffraction patterns corresponding to the engineered feldspar are shown, in which the diffraction peaks correspond mainly to anorthite (JCDPS 86-1705) and zircona (JCDPS 49-1642 and JCDPS 37-1484). The contact time with the saturated solution of lime produces new crystalline phases correlated with the presence of a hydrated aluminosilicate and carboaluminates, 11.1 and 11.7 ˚2θ, respectively (see Figure 3d), in addition of the main feldspar crystalline phases. The higher calcium and Al_2O_3 content in E feldspar favors the formation of these compounds. Portlandite phase is not observed in these XRD patterns. New XRD was carried out in the cement pastes cured more than 28 days, in order to check the phases obtained in the hydrated pastes. Figure 4 shows the XRD patterns of white Porltand cement in comparison with the composites having E feldspar (figure 4a) and M feldspar (figure 4b) substitutions. It can be observed that ettringite, C-S-H gel, quartz, brownmillerite and calcite phases have been formed in all samples. In cements with feldspars substitutions also anorthite and albite phases are shown. However, Portlandite nor appears in these XRD patters. XRD was measured in the range of 10-22º to look for the main peak of Portlandite, but it only appears in sample with 15 wt.% of M feldspar (figure S1 of supporting information). This fact is due to a carbonation effect of cement, which is a natural process that occurs during the ageing of a concrete structure. FTIR analysis was also carried out in these pastes (presented in figure S2 of supporting information) where it is possible to observe that Portlandite peak (~3650 cm-1) doesn't appear but carbonates peak at ~1400-1600 cm-1 does, even in the pure cement sample, verifying this effect [29].

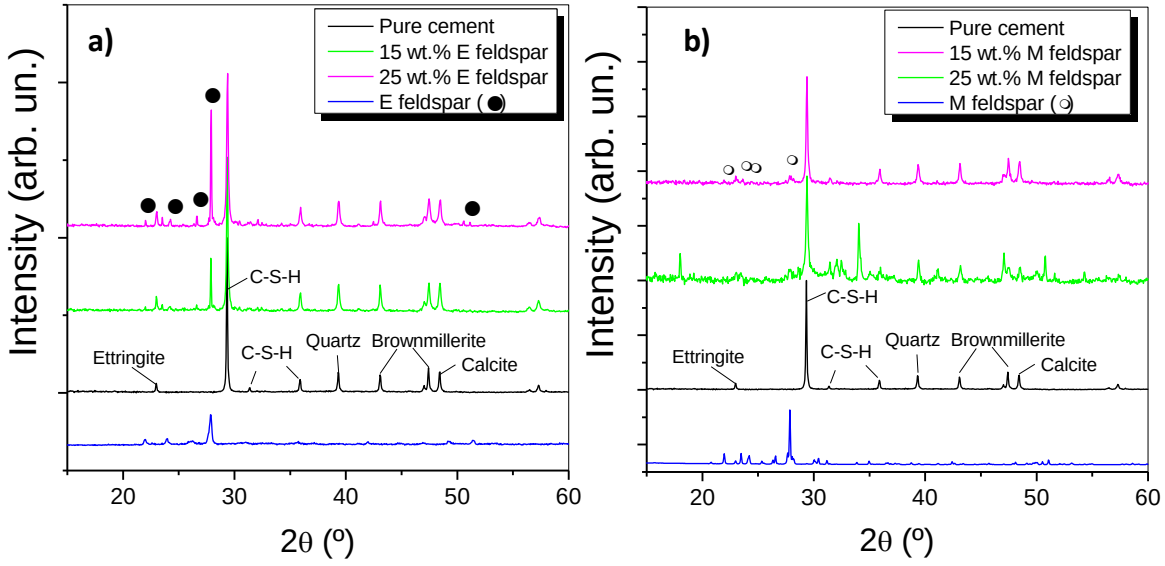

Figure 4: XRD of cement composites in comparison with a) E feldspar substitution cements and a) M feldspar substitution cements. Composites cured after 28 days.

3.2 Functionality properties

The samples consisted of pastes of pure cement and of cement with feldspars substitutions were prepared following the UNE EN 196-1 standard, obtaining samples with apparent densities observed in Table 3, where it is observed that density values are reduced when feldspars are added regarding pure cement. The real density of white cement is 3.15 g/cm^3 and 2.59 g/cm^3 and 2.61 g/cm^3 for E and M feldspars, respectively. Therefore, it is expected that the substitution of cement by these feldspars reduces the total density. The difference between real and apparent density corresponds to the pores volume presents in the pastes. Hence, cement paste possesses 41 vol. % of pores and samples with substitution of 25 wt. % of feldspars possess 43 vol. % and 39 vol. % for E and M feldspar, respectively. Therefore, the pores volume of the three samples are very similar, from which it is inferred that the density reduction observed in Table 3 is mostly due to the effect of introducing a lower density material, not to the pores volume. These physical properties can affect to the functional properties, as will see below, however, the use of these composites as cold coating in façades for reducing the buildings heating, minimizes the importance of these differences of densities.

Table 3. Apparent densities of prepared samples.

	Apparent Density (g/cm^3)
Pure cement	1.86
Cement + 15wt. % M feldspar	1.74
Cement + 25wt. % M feldspar	1.76
Cement + 15wt. % E feldspar	1.83
Cement + 25wt. % E feldspar	1.68

3.2.1 Optical measurements

Reflectance measurements were obtained in all the solar range (UV-Vis-NIR): the UV range gives information about the reflection of the most energetic part of the spectrum and, therefore, the one that greater damages can cause; the visible range gives mainly information about the

whiteness of the sample; and the NIR range gives information about the thermal radiation reflection of the sample. Figure 5 and Table 4 show the reflectance data of samples with different percentage of E and M feldspar for cured samples, 28 days. As seen, in the case of cement with E feldspar, the substitution of 25 wt. % improves the reflectance above cement. The increasing in reflectance affects greatly the NIR range, since E feldspar possesses a larger reflection in the NIR [3], which favors the thermal heating reduction. At the highest cement substitution, part of E feldspar reacts in part with cement and the unreacted part brings its singular properties to the composite, as verified by XRD (figure 4a). This fact is much less pronounced in the 15 wt.% substitution. On the other hand, M feldspar substitution does not modify the reflectance in comparison with pure cement, since it reacts almost entirely with the cement in all proportions (figure 4b). These differences in the reflectance properties are mainly due to the optical behavior of the studied feldspars, since, as seen, the pores volume, which also could provide differences in the light scattering, is very similar in the three samples, so the difference are due to the inherent optical properties of feldspars.

Therefore, the cement substitution by E feldspar in 25 wt. % improves reflectance which will reduce heat transmission, while the M feldspar substitution does not contribute to the overall reflectance of the cement pastes.

Table 4. Average reflectance values of cement compositions with different feldspar substitutions at 28 days.

	Cement	**E feldspar**		**M feldspar**	
Concentration (wt. %)	0	15	25	15	25
Average Reflectance (%) at 28 days	62.8	62.1	73.4	59.4	62.6

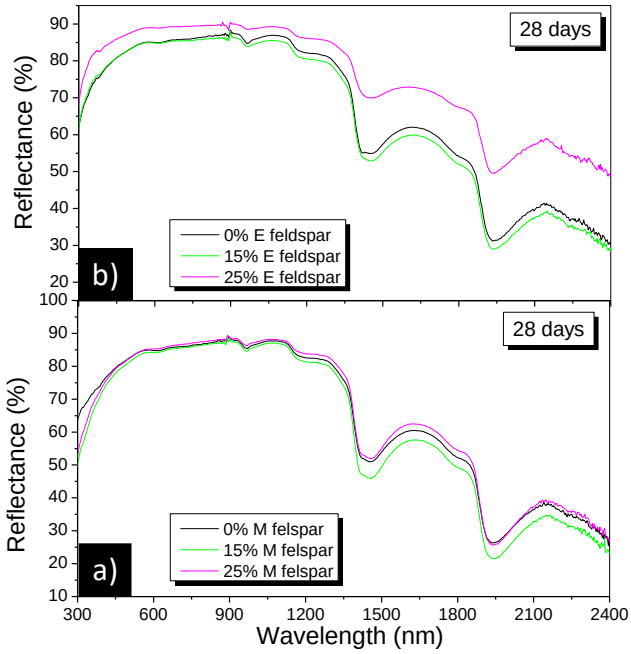

Figure 5: Reflectance curves of cement compositions with different feldspars substitutions: **a)** E feldspar and **b)** M feldspar at 28 days.

In addition, CIEL*a*b* coordinates were measured in order to tabulate in color coordinates the information extracted from de reflectance measurements. Figure 6 presents the CIEL*a*b* coordinates of each sample regarding to the pure cement, that serves as reference for the colorimetric analysis, at the age of 28 days. One of the aim of this work is to improve the whiteness of cement, that is, bring coordinates a* and b* to zero and L* to 100. As seen, E feldspar substitution of 25 wt. % tends to reduce a* and b* coordinates, approaching to zero value and the L* value increases with the E feldspar content, increasing the brightness (figure 6a). However, the M feldspar addition, increases the b* coordinate and hardly varies the L* and a* coordinates at the different feldspar content (figure 6b).

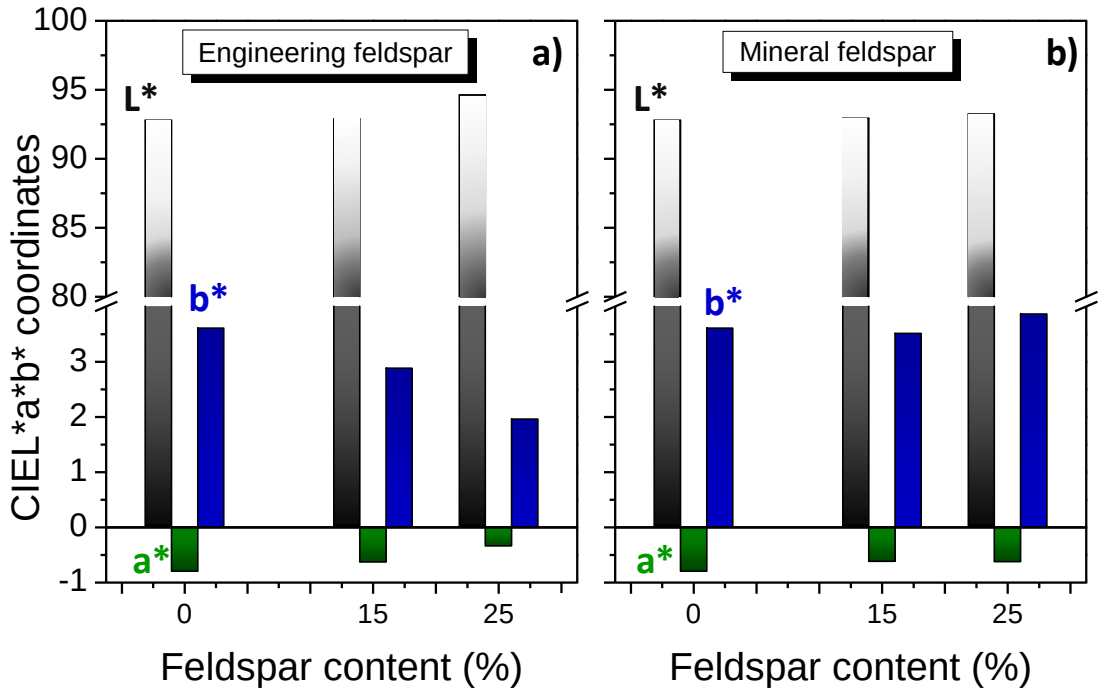

Figure 6. CIEL*a*b* coordinates of cement with different additions of a) E and b) M feldspars at 28 days.

Therefore, when ceramic feldspar substitutes cement in a concentration of 25 wt. %, the whiteness improves greatly that contributes to the higher reflectance and results in better aesthetical response.

3.2.2 Thermal Conductivity

The stationary thermal conductivity of samples was measured in order to compare the thermal behavior and to analyze how the different additions concentrations influence in the cement properties along the aging time [30–32]. The values of thermal conductivity obtained for the cured samples (at 28 days) were 0.59 ± 0.05 W/mK for pure cement and 0.45 ± 0.05 W/mK for all the feldspars substitutions. Therefore, substitution of cement by both feldspars reduces the thermal conductivity regarding the pure cement, due mainly to the lower thermal conductivity of the feldspars, since the pores volume are very similar and does not affect to the conductivity. Moreover, the difference of thermal conductivity when adding both feldspars is not significant due to their similar nature. Although a reduction of 0.14 W/mK may not seem a great improvement, in this values range of thermal conductivity, a small reduction can produce a great improvement in the thermal comfort of a building since the material becomes high thermal insulator, considering it a significant improvement of the thermal properties.

3.2.3 Solar Simulation experiments

Figure 7 shows the results obtained from the solar simulation experiments for samples with different feldspars substitutions cured at 28 days. The sample with higher solar reflectance would show lower heating under solar simulator exposition and, therefore, the temperature gradient should be lower. In case of the E feldspar substitutions, it is observed that the samples achieve lower temperatures than the pure cement, being the sample with 25 wt. % the least heated (Figure 7a). After 5 minutes of irradiation, the 25 wt. % substitution of E feldspar accounts a heating of only 1.8 ºC against the 3.5 ºC observed for the pure cement. In Figures 7b and 7c it is possible to observe the thermal image obtained for the E feldspar composites, where a temperature gradient of 1.8 ºC is registered after 5 min. The M feldspar heating under the same solar exposition is similar than pure cement samples, only variations of 0.4 ºC are observed (Figure 7b). Figures 7e and 7f show the thermal images for the M feldspar composites where the thermal gradient reached after 5 min is 2.7 ºC (similar to pure cement). Moreover, the samples that reach lower temperature gradient will transfer less heat through the sample, although the thermal diffusivity are similar (also the thermal conductivity), as seen in the curves registered in the rear part. This fact makes them a good candidate as cold coatings for buildings façades, reducing the inner heating. In case of M feldspar, the heating transmission is similar than the pure cement.

Therefore, the 25 wt. % substitution of cement by E feldspar provides high solar reflectance that resulted in a reduction of the heating capability under exposition to solar irradiance, making them good candidates for their use as cold coatings for buildings façades.

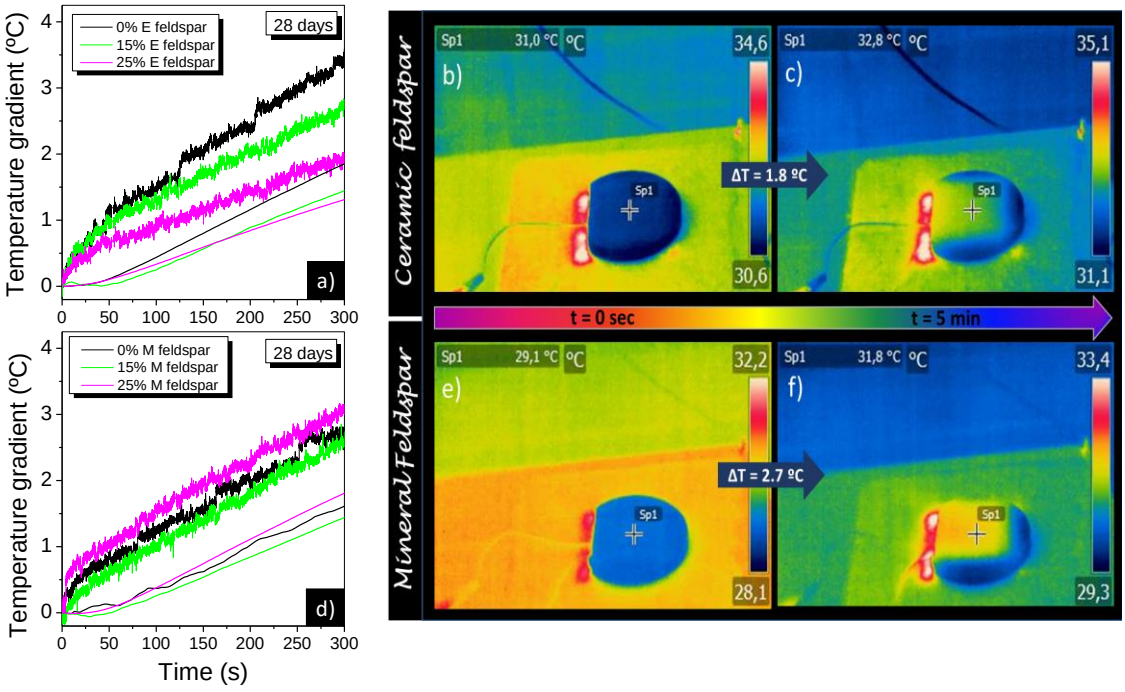

Figure 7. Thermal heating curves under solar simulator exposure for samples with different feldspars substitution and pure cement and infrared images taken with the thermocamera during the experiment for 25 wt.% substitution, at 28 days: engineered ceramic feldspar (**a**, **b** and **c**) and M feldspar (**d**, **e** and **f**). Temperature is expressed as a gradient temperature respect to the initial temperature as a shake of clarity for comparison purposes. Thicker lines correspond to the sample surface temperature monitored by the infrared camera and thin lines correspond to the rear sample surface monitored by a thermocouple. The images were taken at the beginning of the experiment (0 sec) and at the end (5 min).

3.2.4 ASR analysis

The ASR effect can occur in mortars due to the reactions between the high alkali content from cement and silica from the sand of mortars. For this reason, an anticipation of ASR effect was analyzed in cement by the measure of the alkali release in pore solution of samples with 0, 15 and 25 wt. % of glass-ceramic feldspar, after 30 days at room temperature, which would give an idea of the possible posterior reactions with sand. The samples prepared with the natural feldspar were not analyzed due to present lower pozzolanicity, which make them less interesting for applications purposes. The results of the chemical analysis are shown in Table 5. The most important factor in ASR is the silica dissolution which is directly related to the Na^+, K^+, and Ca^{2+} amount in the pore solution, humidity, pH and temperature [33]. Ca^{2+} increase favors the ASR because it is a reagent which also increases the pH of the environment. The pH increase, in turn, favors that, during hydration, OH^- ion attacks the reactive aggregate grains, causing the reactive silica dissolution [17]. Then, this dissolute silica reacts with the alkalis, generating the alkali-silica gel that absorbs water

427 from the surrounding cement paste, swells and induces pressure and expansion causing the
428 cracking of aggregate particles and surrounding paste [16]. In contrast, the presence of aluminum
429 inhibits the ASR because it reduces the silica solubility [34]. Therefore, according to the results
430 observed in table 3, the substitution of cement by the E feldspar produces a decrease in the Ca^{2+}
431 lixiviation up to 75% after 30 days when a 25 wt. % of cement is substituted. The E feldspar
432 possesses lower CaO content than cement, but in the mixture the Ca^{2+} leaching reduction is higher
433 than the corresponding to the 75 wt. % of cement, so a synergistic effect occurs when E feldspar
434 substitutes cement. This reduction of released Ca^{2+} occurs with a solution pH reduction in almost
435 5%, which would avoid, in part, the silica dissolution from the cement. Moreover, the presence of
436 E feldspar introduces Al^{3+} which also inhibits the silica dissolution. The amount of Na^{+} does not
437 vary significantly. On the contrary, K^{+} ions release increases with the E feldspar substitution up to
438 53% at 30 days. However, the total amount of alkalis released in the solution only increases by
439 16% in feldspar substituted cement pastes which is not meaningful for the ASR effect. Finally, in
440 spite of the increase of the amount of silica dissolved when cement is substituted by E feldspar,
441 this increase is less than what should occur with increasing the total amount of silica in the
442 composition due the substitution, because of the inhibit combined effect mentioned above (less
443 Ca^{2+} release and presence of Al^{3+}). Moreover, this dissolved silica does not produce an increase
444 in the ASR because it comes from the aluminosilicate rather than cement, making it less reactive.
445 Furthermore, the total alkalis content, in all cases, is remarkably similar, so the possible creation of
446 alkali-silica gel is the same in the three samples and no difference are observed in their expansion
447 effect.
448 In summary, the substitution of cement by the E feldspar kept the ASR effect in spite of the alkaline
449 content. The lower CaO content of the E feldspar, the same amount of alkalis released in the
450 solution, which, despite of the silica dissolution is larger, produce the same amount of the alkali-
451 silica gel and, therefore, the same expansion than in the pure cement.
452
453 **Table 5.** Concentration of alkali release in pore solution after 30 days.

Engineered feldspar content (%)	SiO_2 (mg/l)	CaO (mg/l)	Na_2O (mg/l)	K_2O (mg/l)	Al_2O_3 (mg/l)	pH
0%	0.82	990	23.0	9.8	0.40	13.20
15%	1.20	565	25.0	12.8	1.80	13.01
25%	5.60	245	19.0	18.3	3.25	12.56

454

4. Cement application for façade coating: experimental test

The cement application by coating a building brick with the different composites simulating a coating for façades was characterized by the same methods than the above pastes samples. Figure 8 shows the heating under solar irradiance monitored by the thermography. After 5 minutes of irradiance the surface of coating having 25 wt. % of E feldspar substitution (Figures 8e, 8f and 8g) register only 1 ºC of heating. This heating is 1.9 ºC lower than pure cement coating (Figures 8a, 8b and 8g) and 1.1 ºC lower than the coating having 25 wt. % of M feldspar (Figures 8b, 8c and 8g). It worth to note that differences of 1ºC inside a building can provide an energy saving of 20% in the acclimatization [35,36]. Moreover, the temperature in the rear of the coated brick under the solar irradiance kept unaltered during the experiment for the 25 wt. % substitution of E feldspar while for the other two samples, the rear part is heated more than 1 ºC (Figure 8g). Moreover, long time experiments (irradiating 6h) have been carried out in order to check whether the behavior is maintained over time. Figure 8h shows the heating curves from 15 min to 360min at the samples surfaces (line with points) and at the rear part (dotted lines). As seen, the heating begins to stabilize around the 2h for the three samples, however, the E feldspar substitution cement achieves lower temperatures both at the surface (ΔT =13.2 ºC) and at the rear part (ΔT =10.4 ºC) than the M feldspar substitution cement (ΔT =14.0 ºC at the surface and ΔT =11.6 ºC at the rear) and, specially, than the pure cement (ΔT =15.4 ºC at the surface and ΔT =14.0 ºC at the rear). So, a relevant reduction of the heating after 6 hours of solar irradiance with one sun equivalent power is demonstrated for a E feldspar composite having a 2.2 ºC reduction for the surface and 3.8 ºC for the rear part of the brick as compared with the white cement coating. The great reduction in thermal heating through the façade makes this material relevant for exterior insulation and finish system (EIFS). As explained, this difference is due to higher reflectance of the E feldspar composite. This fact constitutes an interesting approach to reduce heating in façades by using engineered feldspar as a pozzolanic substitution in cementitious based coatings. Finally, Figure 8i shows a photograph of the application sample where it is observed the brick and the cement coating.

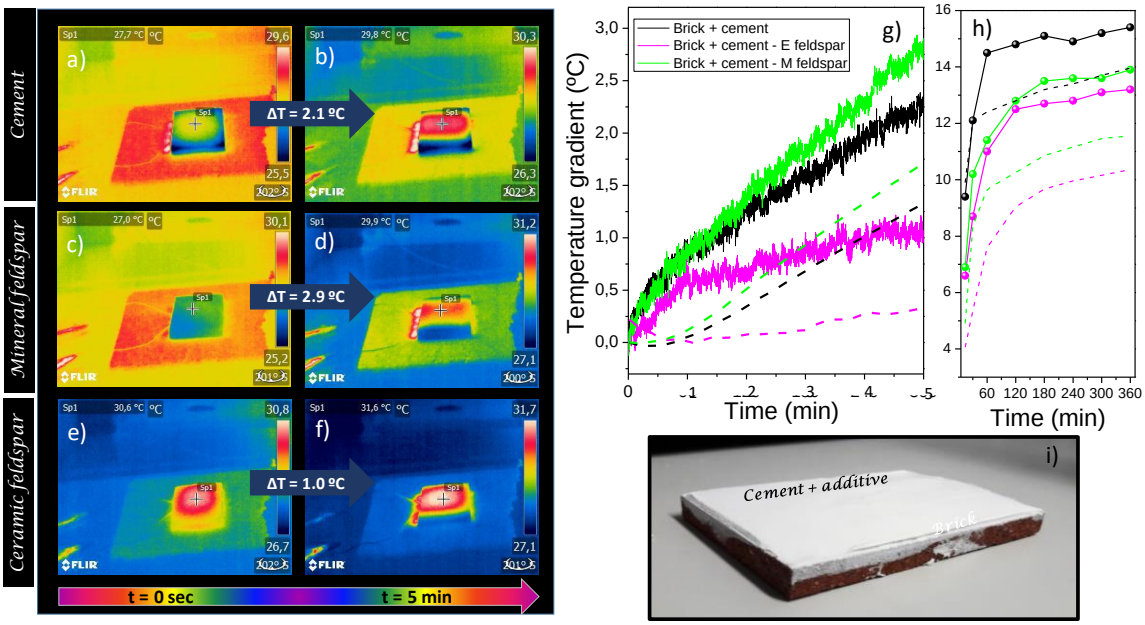

483

484 **Figure 8.** Infrared images taken with the thermocamera during the experiment for
485 application samples composed by a brick coated with cement (**a** and **b**), cement with 25% of M
486 feldspar (**c** and **d**) and cement with 25% of ceramic feldspar (**e** and **f**), at 28 days of aging. The
487 images were taken at the beginning of the experiment (0 sec) (**a, c** and **e**) and at the end (5 min)
488 (**b, d** and **f**). **g**) Heating curves of the surface and the rear part of samples, obtained by the
489 thermocamera and the thermocouple, respectively, at short times and **h)** at long times**. i)**
490 Photograph of the application sample where it is observed the brick and the cement coating.
491
492 The thermal conductivities of these application samples are also measured and are
493 presented in Table 6, in comparison to the brick thermal conductivity. As seen, the brick thermal
494 conductivity is the lowest value due to its high porosity. For M feldspar, the thermal conductivity is
495 slightly reduced regarding to cement. However, the thermal conductivity is almost reduced to a half
496 in case of composite with engineered feldspar substitution, achieving very low values for this kind
497 of building materials, close to the departure brick. These results are very outstanding taking into
498 account that the composite coating is only of 0.4 cm in thickness. Moreover, the results agree with
499 those obtained in the simulation experiments, showing a significant improvement of the thermal
500 properties for sample with ceramic feldspar substitution. These results along to the high reflectivity
501 of cement with E feldspar open the possibility of using this new material in buildings in order to
502 reduce the heat impact over façades which could reduce the energy needed to acclimate the inner,
503 promoting sustainable buildings and also supposes a reduction of material cost since, as seen,
504 only thin coatings are necessary to obtain good results.

505

506

507 **Table 6.** Thermal conductivity of cement coated

Sample	Thermal conductivity (W/mK) (28 days) (± 0.05)
Brick	0.36
Brick + Cement coating	0.85
Brick + Cement with M feldspar 25 wt. % coating	0.74
Brick + Cement with E feldspar 25 wt. % coating	0.46

508

509 ## 5. Conclusions

510 New additions based on feldspars (mineral, M, and engineered, E) have been successfully
511 incorporated in white cement in different concentrations to substitute it. These additions have
512 resulted profitable because of the great availability of this kind of materials in the earth and, in
513 addition, for the improvement of the composites properties. The calcium content and the
514 characteristic of these feldspars, have allowed having a pozzolanic activity in the cement
515 composites which maintains the mechanical and chemical requirements of cements. In addition,
516 the cements substituted by the engineered feldspar do not present larger alkali release than pure
517 cement, which could produce posterior ASR effects in mortars, despite the larger amount of alkalis
518 in the feldspar, due to the presence of alumina, the lower amount of CaO and the same amount of
519 alkalis released to the solution, which generate the same expansion effects than in pure cement.
520 Moreover, due to the exceptional properties of these feldspars, especially for the synthetized one,
521 cement has been provided with improved thermal and optical properties. The high reflectance and
522 low thermal conductivity of the engineered feldspar, have allowed that cement composites with 25
523 wt.% of this feldspar has increases its reflectance, especially in the NIR, increasing also its
524 whiteness and has reduced the thermal diffusivity, which minimizes the heat transmission through
525 the sample. The values obtained for the engineered feldspar highlight over the mineral feldspar,
526 that, although provides an improvement of the composite properties, does not reach such good
527 results. For all these characteristics, larger puzzolanity, lower ASR effect, higher reflectance and
528 lower thermal conductivity, this cement composite with engineered feldspar could be a promising
529 material for sustainable buildings, since it could provide high reflective façades and high energy
530 saving, reducing the impact of heat islands in the cities.

Acknowledgements:

The authors express their thanks to the Project MAT-2017-86450-C4-1-R, CSIC NANOMIND project CSIC2015-60E068 and projects CDTI (IDI-20130894 and IDI-20161120) for their financial support. Dra. E. Enriquez is also indebted to MINECO for a ‘‘Torres Quevedo’’ contract (ref: PTQ-14-07289), which is co-financed with European Social Funds.

References:

[1] A. Antonaia, F. Ascione, A. Castaldo, A. D'Angelo, R.F. De Masi, M. Ferrara, G.P. Vanoli, G. Vitiello, Cool materials for reducing summer energy consumptions in Mediterranean climate: In-lab experiments and numerical analysis of a new coating based on acrylic paint, Appl. Therm. Eng. 102 (2016) 91–107. doi:10.1016/j.applthermaleng.2016.03.111.

[2] M. Santamouris, Cooling the cities – A review of reflective and green roof mitigation technologies to fight heat island and improve comfort in urban environments, Sol. Energy. 103 (2014) 682–703. doi:10.1016/j.solener.2012.07.003.

[3] E. Enríquez, V. Fuertes, M.J. Cabrera, J. Seores, D. Muñoz, J.F. Fernández, New strategy to mitigate urban heat island effect: Energy saving by combining high albedo and low thermal diffusivity in glass ceramic materials, Sol. Energy. 149 (2017). doi:10.1016/j.solener.2017.04.011.

[4] R. Levinson, P. Berdahl, A. Asefaw Berhe, H. Akbari, Effects of soiling and cleaning on the reflectance and solar heat gain of a light-colored roofing membrane, Atmos. Environ. 39 (2005) 7807–7824. doi:10.1016/j.atmosenv.2005.08.037.

[5] C. Ferrari, A. Libbra, A. Muscio, C. Siligardi, Design of ceramic tiles with high solar reflectance through the development of a functional engobe, Ceram. Int. 39 (2013) 9583–9590. doi:10.1016/j.ceramint.2013.05.077.

[6] A. Laura, A.D. Alessandro, S. Sambuco, M. Rallini, F. Ubertini, F. Asdrubali, A. Luigi, F. Cotana, Multipurpose experimental characterization of smart nanocomposite cement-based materials for thermal-energy e ffi ciency and strain-sensing capability, Sol. Energy Mater. Sol. Cells. 161 (2017) 77–88. doi:10.1016/j.solmat.2016.11.030.

[7] C. Udawattha, H. Galabada, R. Halwatura, Mud concrete paving block for pedestrian pavements, Case Stud. Constr. Mater. 7 (2017) 249–262. doi:10.1016/j.cscm.2017.08.005.

561 [8] F. Puertas, S. Goñi, M.S. Hernández, C. Varga, A. Guerrero, Comparative study of
562 accelerated decalcification process among C3S, grey and white cement pastes, Cem.
563 Concr. Compos. 34 (2012) 384–391. doi:10.1016/j.cemconcomp.2011.11.002.

564 [9] A.P. Kirchheim, V. Rheinheimer, D.C.C. Dal Molin, Comparative study of white and ordinary
565 concretes with respect of carbonation and water absorption, Constr. Build. Mater. 84 (2015)
566 320–330. doi:10.1016/j.conbuildmat.2015.03.020.

567 [10] M.E.S.I. Saraya, Study physico-chemical properties of blended cements containing fixed
568 amount of silica fume, blast furnace slag, basalt and limestone, a comparative study, Constr.
569 Build. Mater. 72 (2014) 104–112. doi:10.1016/j.conbuildmat.2014.08.071.

570 [11] M. Frias, M.I. Sánchez De Rojas, J. Santamaría, C. Rodríguez, Recycling of
571 silicomanganese slag as pozzolanic material in Portland cements: Basic and engineering
572 properties, Cem. Concr. Res. 36 (2006) 487–491. doi:10.1016/j.cemconres.2005.06.014.

573 [12] Y. Kocak, S. Nas, The effect of using fly ash on the strength and hydration characteristics
574 of blended cements, Constr. Build. Mater. 73 (2014) 25–32.
575 doi:10.1016/j.conbuildmat.2014.09.048.

576 [13] Y. Senhadji, G. Escadeillas, M. Mouli, H. Khelafi, Benosman, Influence of natural pozzolan,
577 silica fume and limestone fine on strength, acid resistance and microstructure of mortar,
578 Powder Technol. 254 (2014) 314–323. doi:10.1016/j.powtec.2014.01.046.

579 [14] M.M. Hossain, M.R. Karim, M. Hasan, M.K. Hossain, M.F.M. Zain, Durability of mortar and
580 concrete made up of pozzolans as a partial replacement of cement: A review, Constr. Build.
581 Mater. 116 (2016) 128–140. doi:10.1016/j.conbuildmat.2016.04.147.

582 [15] M.M. Hossain, M.R. Karim, M.K. Hossain, M.N. Islam, M.F.M. Zain, Durability of mortar and
583 concrete containing alkali-activated binder with pozzolans: A review, Constr. Build. Mater.
584 93 (2015) 95–109. doi:10.1016/j.conbuildmat.2015.05.094.

585 [16] Z. Owsiak, J. Zapała-Sławeta, P. Czapik, Diagnosis of concrete structures distress due to
586 alkali-aggregate reaction, Bull. Polish Acad. Sci. Tech. Sci. 63 (2015) 23–29.
587 doi:10.1515/bpasts-2015-0003.

588 [17] J. Feiteira, J. Custódio, M.S.S. Ribeiro, Review and discussion of polymer action on alkali-
589 silica reaction, Mater. Struct. Constr. 46 (2013) 1415–1427. doi:10.1617/s11527-012-9983-
590 2.

591 [18] Asociación Española de Normalización y certificación, EN 196-5. Method of Testing
592 Cement. Part 5: Pozzolanicity Test for Pozzolanic Cement. AENOR., Spain, 2011.

593 [19] E. Asensio, C. Medina, M. Frías, M.I.S. de Rojas, Characterization of Ceramic-Based
594 Construction and Demolition Waste: Use as Pozzolan in Cements, J. Am. Ceram. Soc. 99
595 (2016) 4121–4127. doi:10.1111/jace.14437.

596 [20] UNE-EN 196-5. Métodos de ensayo de cementos. Ensayo de puzolanicidad para los
597 cementos puzolánicos, 2011.

598 [21] M.I.S. de Rojas, M. Frias, J. Rivera, M.J. Escorihuela, F.P. Marin, Research about the
599 pozzolanic activity of waste materials from calcined clay, Mater. Constr. 51 (2001) 45–52.

600 [22] M.P. Luxán, M.I. Sánchez de Rojas, M. Frías, Investigations on the fly ash-calcium
601 hydroxide reactions, Cem. Concr. Res. 19 (1989) 69–80. doi:10.1016/0008-
602 8846(89)90067-7.

603 [23] M.I. Sánchez De Rojas, M. Frías, The pozzolanic activity of different materials, its influence
604 on the hydration heat in mortars, Cem. Concr. Res. 26 (1996) 203–213. doi:10.1016/0008-
605 8846(95)00200-6.

606 [24] J.M. Medina, I.F. Sáez Del Bosque, M. Frías, M.I. Sánchez de Rojas, C. Medina,
607 Characterisation and valorisation of biomass waste as a possible addition in eco-cement
608 design, Mater. Struct. 50 (2017) 1–13. doi:10.1617/s11527-017-1076-9.

609 [25] I. García Lodeiro, A. Fernández-Jimenez, A. Palomo, D.E. Macphee, Effect on fresh C-S-H
610 gels of the simultaneous addition of alkali and aluminium, Cem. Concr. Res. 40 (2010) 27–
611 32. doi:10.1016/j.cemconres.2009.08.004.

612 [26] I. García Lodeiro, D.E. Macphee, A. Palomo, A. Fernández-Jiménez, Effect of alkalis on
613 fresh C-S-H gels. FTIR analysis, Cem. Concr. Res. 39 (2009) 147–153.
614 doi:10.1016/j.cemconres.2009.01.003.

615 [27] R. Ylmén, U. Jäglid, B.M. Steenari, I. Panas, Early hydration and setting of Portland cement
616 monitored by IR, SEM and Vicat techniques, Cem. Concr. Res. 39 (2009) 433–439.
617 doi:10.1016/j.cemconres.2009.01.017.

618 [28] M. Torres-carrasco, A. Campo, M.A. De Rubia, E. Reyes, A. Moragues, J.F. Fernández,
619 New insights in weathering analysis of anhydrous cements by using high spectral and
620 spatial resolution Confocal Raman Microscopy, Cem. Concr. Res. 100 (2017) 119–128.

621 [29] R. Ylmén, U. Jäglid, Carbonation of Portland Cement Studied by Diffuse Reflection Fourier
622 Transform Infrared Spectroscopy, Int. J. Concr. Struct. Mater. 7 (2013) 119–125.
623 doi:10.1007/s40069-013-0039-y.

624 [30] R.R. Krishnamoorthy, J.A. Zujip, Thermal Conductivity and Microstructure of Concrete
625 Using Recycle Glass as a Fine Aggregate Replacement, Int. J. Emerg. Technol. Adv. Eng.
626 3 (2013) 463–471.

627 [31] M.Z. Guo, Z. Chen, T.C. Ling, C.S. Poon, Effects of recycled glass on properties of
628 architectural mortar before and after exposure to elevated temperatures, J. Clean. Prod.
629 101 (2015) 158–164. doi:10.1016/j.jclepro.2015.04.004.

630 [32] A. Alani, J. MacMullen, O. Telik, Z.Y. Zhang, Investigation into the thermal performance of
631 recycled glass screed for construction purposes, Constr. Build. Mater. 29 (2012) 527–532.
632 doi:10.1016/j.conbuildmat.2011.07.020.

633 [33] S.G. Wood, E.R. Giannini, M.A. Ramsey, R.D. Moser, Autoclave test parameters for
634 determining alkali-silica reactivity of concrete aggregates, Constr. Build. Mater. 168 (2018)
635 683–691. doi:10.1016/j.conbuildmat.2018.02.114.

636 [34] T. Chappex, K.L. Scrivener, The effect of aluminum in solution on the dissolution of
637 amorphous silica and its relation to cementitious systems, J. Am. Ceram. Soc. 96 (2013)
638 592–597. doi:10.1111/jace.12098.

639 [35] R. Levinson, H. Akbari, P. Berdahl, Measuring solar reflectance-Part I: Defining a metric
640 that accurately predicts solar heat gain, Sol. Energy. 84 (2010) 1717–1744.
641 doi:10.1016/j.solener.2010.04.018.

642 [36] M. Zinzi, Characterisation and assessment of near infrared reflective paintings for building
643 facade applications, Energy Build. 114 (2015) 206–213. doi:10.1016/j.enbuild.2015.05.048.

644